Rogue waves for a long wave-short wave resonance model with multiple short waves

Hiu Ning Chan [(1)], Edwin Ding [(2)], David Jacob Kedziora [(3)], Roger Hamilton James Grimshaw [(4)], Kwok Wing Chow [(1)*]

(1) = Department of Mechanical Engineering, University of Hong Kong Pokfulam, Hong Kong

(2) = Department of Mathematics and Physics, Azusa Pacific University, Azusa, CA 91702, USA

(3) = Research School of Physics and Engineering, Australian National University, Canberra ACT 0200, Australia

(4) = Department of Mathematical Sciences, Loughborough University, Loughborough LE11 3TU, United Kingdom

* = Corresponding author

Email: kwchow@hku.hk **Phone**: (852) 2859 2641 **Fax**: (852) 2858 5415

NODY-D-14-00252

Re-submission date: **April 2016**

Keywords: Rogue waves; Long-short resonance

PACS Classification: 02.30.Jr; 05.45.Yv; 47.35.Fg

ABSTRACT

A resonance between long and short waves will occur if the phase velocity of the long wave matches the group velocity of the short wave. In this paper, a system with two distinct packets of short waves in resonance with a common long wave is studied. Breather solutions are calculated by the Hirota bilinear method, and rogue wave modes (unexpectedly large displacements from an otherwise calm background state) are obtained from the breathers through a long wave limit. The location and magnitude of the maximum displacement are determined quantitatively. Remarkably this coupling enables a rogue wave to attain a larger magnitude than that in a configuration with just one single short wave component. Furthermore, as the wavenumber varies, a transition from an elevation rogue wave to a depression rogue wave is possible. This transformation of the wave profile is elucidated in terms of the properties of the carrier envelope. The connection with the modulation instability of the background plane wave is investigated. Some numerical simulations are performed to demonstrate both the robust nature and unstable behavior for these rogue waves, depending on the parameters of the system. Dynamics and properties of rogue waves with three or more short wave components are also considered.

1 Introduction

Three-wave resonance is important in many areas of physics, such as fluid dynamics [1] and optics [2]. From a general perspective, in any nonlinear wave system with a linear dispersion relation $\omega = \omega(k)$ (ω = angular frequency, k = wavenumber), if three wave components satisfy the resonance conditions:

$$\omega_3 = \omega_1 + \omega_2, \quad k_3 = k_1 + k_2,$$

then one member of such a triad can be generated spontaneously if two other members are present. The 'long wave-short wave' (or just 'long-short') resonance is a special limiting case of the triad resonance when one member is much longer than the other two [1, 3]. Specifically, if $k_1 = k$, $k_2 = \Delta k$, $k_3 = k + \Delta k$, then the resonance condition becomes $\omega(k + \Delta k) = \omega(k) + \omega(\Delta k)$, which to leading order reduces to

$$\frac{\omega(\Delta k)}{\Delta k} \approx \frac{d\omega(k)}{dk}$$

when $|\Delta k| << k$, i.e. the phase velocity of the long wave must match the group velocity of the short wave. Under such circumstances, a standard multiple scale asymptotic expansion will give the governing equations of a slowly varying, complex-valued short wave packet envelope (S) and a real-valued induced long wave (L) as [3, 4],

$$iS_t - S_{xx} = LS\,,\ \ L_t = -\,\sigma(|S|^2)_x\,. \tag{1}$$

The real parameter σ will depend on the specific physical application. The resonance between a long internal wave and a short surface wave in a stratified fluid is one important application, but the model Eq. (1) applies to many other physical systems.

Exact solutions of Eq. (1) with interpretation as bright and dark solitons have been given, see [5] for instance. The objective of the present work is to take these studies further. More specifically, we shall investigate rogue waves for waveguides consisting of such a coupled long-short system with multiple short waves.

Rogue waves (or freak waves) are unexpectedly large displacements from the background state. Typically these modes are localized in both space and time. Although such large amplitude motions have been known to the maritime community for several decades, scientific interest has exploded in the past ten years with the availability of new ocean and laboratory data, all leading to the realization that the nonlinear Schrödinger equation could play a central role in modeling these events. The analytical and experimental identification of the counterparts in optical waveguides have only strengthened these topical appeals [6]. Indeed rogue waves have been invoked in many scientific disciplines, ranging from crowd dynamics [7] to tunneling in waveguides with graded index [8].

The most widely used model is the Peregrine breather/rogue wave [9] solution of the focusing nonlinear Schrödinger equation, for which plane waves are modulationally unstable. This rogue wave is localized in both space and time (i.e. it breathes only once), and decays algebraically to the background state. Recently studies of rogue waves have been extended to systems with two or more waveguides, i.e. those governed by coupled systems, e.g. Bose-Einstein condensates [10, 11], optical fibers [12], and even modeling in finance [13]. Rational solutions are still obtained [14].

The Darboux transformation has been commonly used in the theoretical search for rogue waves, but the classical Hirota method has also recently been shown to be applicable [15]. The merit of the Hirota method is that it has been successfully employed in the theory of nonlinear waves to search for soliton modes for over forty years [16]. Given this, we note that the Darboux transformation has been applied to the single component long-short system Eq. (1) to obtain a 'dark' rogue wave, an unexpected 'depression' from the background state [17]. It would thus be instructive to study the combination of modes in a coupled system with two (or more) components, i.e. elevation rogue wave in one waveguide but a depression rogue wave in the other. The Hirota method will be an effective tool in such

investigations. Nevertheless, in anticipation for future studies, the Lax pairs for such coupled systems will be formulated too.

Modulation instability (MI) refers to the general process whereby sidebands of the central wavenumber in the wave packet grow in a nonlinear system. As the system evolves, nonlinear effects play a central role, and this relationship connecting MI, breather and rogue wave has been studied in the literature, see e.g. [18]. The structural stability of a rogue wave mode can also be investigated from the perspective of MI.

The structure of the paper is now described. The Hirota bilinear transform and the Lax pair of a coupled long-short system will be formulated, and the breather mode will be computed by the bilinear method (Section 2). A long wave limit is then taken and the rogue wave is obtained (Section 3). The transformation of the wave profile, from an elevation to a depression rogue wave mode, will be traced analytically (Section 4). Many varieties in the combination of modes will be investigated further in Section 5. MI and numerical simulations will be discussed (Section 6). Extension to a general multi-component system will be discussed in Section 7, followed by the Conclusions (Section 8).

2 Formulation

A system consisting of two short wave components, each in resonance with a common long wave, is considered in a general theoretical setting. In terms of applications in a fluid dynamics context, two wave packets in a stratified fluid are coupled to the induced mean flow (long wave) of the system. The constraint is that the group velocities of the two short wave packets must be identical, and in this group velocity frame the governing equations become

$$iA_t - A_{xx} = LA \ , \ iB_t - B_{xx} = LB \ , \ L_t = -\sigma(|A|^2 + |B|^2)_x \ , \tag{2}$$

where A, B, L are the short waves and long wave respectively [1, 19]. The real parameter σ depends on the precise physical properties of the system, e.g. the density stratification profile in a fluid. Although it can be normalized to unity by changes of variables, we retain it here as a useful measure of the long-short wave interaction. The scattering and eigenvalue problems of Eq. (2) have been studied, and localized solitons have been derived [18]. The system is conservative, and one representation of the intensity or energy of each mode, namely,

$$\int |A|^2 dx, \int |B|^2 \, dx, \int L dx \ , \tag{3}$$

remains constant. The focus of this paper is to study the breather and rogue wave modes of Eq. (2). Both the Hirota bilinear transform and Lax pair formulations will be developed, and the breather mode will be computed from the former.

The Hirota bilinear formulation

The well established Hirota bilinear transformation is given by:

$$D_x^m D_t^n g \cdot f = \left(\frac{\partial}{\partial x} - \frac{\partial}{\partial x'} \right)^m \left(\frac{\partial}{\partial t} - \frac{\partial}{\partial t'} \right)^n g(x,t) f(x',t') \Big|_{x=x', t=t'} . \quad (4)$$

The appropriate dependent variable transformation is (G, H complex, f real)

$$A = \frac{G}{f}, B = \frac{H}{f}, L = \left(2 \log f \right)_{xx}, \quad (5)$$

which converts Eq. (2) to

$$\left(iD_t - D_x^2 \right) G \cdot f = 0, \left(iD_t - D_x^2 \right) H \cdot f = 0, \left(D_x D_t - C \right) f \cdot f = -\sigma \left(|G|^2 + |H|^2 \right). \quad (6)$$

The breather (pulsating) solutions are now derived, using complex conjugate wavenumbers. The two possible types of breathers, namely, those periodic in space and those periodic in time, can be attained through a suitable choice of wavenumbers. Rogue waves are then obtained by taking the long wave limit of these breathers.

We avoid the trivial case of identical short wave components by insisting on distinct carrier wave envelopes,

$$G = \rho \exp\left[i\left(kx - \omega t \right) \right] g, H = \rho h, \ \omega = -k^2, \ k \neq 0, \quad (7)$$

where k, ω, ρ stand for (real valued) wavenumber, angular frequency and wave amplitude respectively. For simplicity attention is restricted to the case of equal background amplitude for both short waves. The case of unequal amplitudes will be left for future studies. The appropriate expansion is then (* = complex conjugate)

$$\begin{aligned} f &= 1 + \exp\left(px - \Omega t + \zeta^{(1)}\right) + \exp\left(p^* x - \Omega^* t + \zeta^{(2)}\right) \\ &\quad + M \exp\left[(p + p^*)x - (\Omega + \Omega^*)t + \zeta^{(1)} + \zeta^{(2)}\right], \\ g &= 1 + a_1 \exp\left(px - \Omega t + \zeta^{(1)}\right) + a_2 \exp\left(p^* x - \Omega^* t + \zeta^{(2)}\right) \\ &\quad + M a_1 a_2 \exp\left[(p + p^*)x - (\Omega + \Omega^*)t + \zeta^{(1)} + \zeta^{(2)}\right], \\ h &= 1 + b_1 \exp\left(px - \Omega t + \zeta^{(1)}\right) + b_2 \exp\left(p^* x - \Omega^* t + \zeta^{(2)}\right) \\ &\quad + M b_1 b_2 \exp\left[(p + p^*)x - (\Omega + \Omega^*)t + \zeta^{(1)} + \zeta^{(2)}\right]. \end{aligned} \tag{8}$$

Substituting into the bilinear forms (Eq. (6)) will yield

$$a_1 = \frac{i(\Omega + 2kp) - p^2}{i(\Omega + 2kp) + p^2},\ a_2 = \frac{i(\Omega^* + 2kp^*) - (p^*)^2}{i(\Omega^* + 2kp^*) + (p^*)^2},$$

$$b_1 = \frac{i\Omega - p^2}{i\Omega + p^2},\ b_2 = \frac{i\Omega^* - (p^*)^2}{i\Omega^* + (p^*)^2},$$

$$M = \frac{(p^*\Omega - p\Omega^*)^2 + [pp^*(p - p^*)]^2}{(p^*\Omega - p\Omega^*)^2 + [pp^*(p + p^*)]^2}. \tag{9}$$

In contrast to the single mode case, the dispersion relation is now a polynomial of degree five (rather than degree three),

$$-\sigma\rho^2 = \frac{\Omega\left(\Omega^2 + p^4\right)\left\{\left(\Omega + 2kp\right)^2 + p^4\right\}}{4p^3\left(\Omega^2 + 2kp\Omega + 2k^2p^2 + p^4\right)} \,. \tag{10}$$

For $k = 0$, we have $A = B$ and this whole analysis then degenerates to a scenario equivalent to the single component case. Eq. (2) simplifies to

$$iA_t - A_{xx} = LA \,,\; L_t = -2\sigma(|A|^2)_x \,, \tag{11}$$

which is equivalent to Eq. (1) except the parameter is now 2σ. The dispersion relation Eq. (10) also reduces to a cubic polynomial similar to results published earlier [15].

The Lax pair formulation

It is widely believed that the integrability of nonlinear evolution equations, the existence of an infinite number of conservation laws and the Lax pair are closely related. It is thus highly valuable to find a Lax pair representation of the system Eq. (2). This involves searching for matrices U and V such that the partial differential equations

$$R_x = U \cdot R, \;\; R_t = V \cdot R$$

reduce to the original nonlinear system under the compatibility condition $R_{xt} = R_{tx}$ or the associated zero-curvature equation $U_t - V_x + [U,V] = 0$, where the commutator is defined as $[U,V] = UV - VU$.

More precisely, the matrices

$$U = \begin{bmatrix} i\lambda & \sqrt{\frac{\sigma_2 f_i}{2 f_d^2}} B & \sqrt{\frac{\sigma_1 f_i}{2 f_d^2}} A & -i\frac{f_i}{f_d} L \\ 0 & 0 & 0 & -\sqrt{\frac{\sigma_1 f_i}{2 f_d^2}} B^* \\ 0 & 0 & 0 & -\sqrt{\frac{\sigma_1 f_i}{2 f_d^2}} A^* \\ -i & 0 & 0 & -i\lambda \end{bmatrix},$$

$$V = \begin{bmatrix} -\frac{i}{2} f_d \lambda^2 & \sqrt{\frac{\sigma_2 f_i}{2}} \left(iB_x - \lambda B\right) & \sqrt{\frac{\sigma_1 f_i}{2}} \left(iA_x - \lambda A\right) & -i\frac{f_i}{2 f_d} \left(\sigma_1 |A|^2 + \sigma_2 |B|^2\right) \\ -\sqrt{\frac{\sigma_2 f_i}{2}} B^* & \frac{i}{2} f_d \lambda^2 & 0 & \sqrt{\frac{\sigma_2 f_i}{2}} \left(iB_x^* - \lambda B^*\right) \\ -\sqrt{\frac{\sigma_1 f_i}{2}} A^* & 0 & \frac{i}{2} f_d \lambda^2 & \sqrt{\frac{\sigma_1 f_i}{2}} \left(iA_x^* - \lambda A^*\right) \\ 0 & \sqrt{\frac{\sigma_2 f_i}{2}} B & \sqrt{\frac{\sigma_1 f_i}{2}} A & -\frac{i}{2} f_d \lambda^2 \end{bmatrix}$$

are the appropriate choices to give the generalized system

$$iA_t + f_d A_{xx} + f_i LA = 0,$$

$$iB_t + f_d B_{xx} + f_i LB = 0,$$

$$L_t = (\sigma_1 AA^* + \sigma_2 BB^*)_x,$$

where the constant f_d determines the strength of dispersion, the constant f_i determines the strength of the nonlinear long wave-short wave interaction, and the constants σ_1 and σ_2 measure the relative weight of this interaction between the

short wave components. As before, changes of variables can be made to normalize both σ_1 and σ_2.

While arbitrary coupling schemes do not guarantee integrability, it is noteworthy that this generalized system can be extended to any number of components, essentially by replacing the scalar short-wave function in the single-component Lax pair [15] with a vector field. Lax pairs are generally very important entities, as they form the basis of many ingenious methods for constructing solutions explicitly [20]. A particular selection of parameters, namely, $f_d = f_i = -1$, $\sigma_1 = \sigma_2 = -\sigma$, will give the resonance equations Eq. (2). Although the Hirota formulation is sufficient for the present work, the Lax pair mechanism will form the foundation for further theoretical development in the future.

3 Rogue waves of the coupled long-short system

Although one should in principle analyze the dispersion relation Eq. (10) for arbitrary complex wavenumber p, it will be instructive to obtain the breather solution for a purely imaginary value, namely,

$p = ip_0$, where p_0 is a real number, (12)

since such a solution corresponds to a breather strictly periodic in the x direction, commonly known as the Akhmediev breather in the literature [21]. The asymptotic expansion for Ω in that case is

$\Omega = p_0\left[\Omega_0 + O\left(p_0^2\right)\right]$, where Ω_0 satisfies

$$\Omega_0^5 + 4ki\Omega_0^4 - 4k^2\Omega_0^3 - 4\sigma\rho^2 i\Omega_0^2 + 8\sigma\rho^2 k\Omega_0 + 8\sigma\rho^2 k^2 i = 0\,. \tag{13}$$

Performing now a long wave expansion ($p_0 \to 0$), with the phase factors $\exp(\zeta^{(n)}) = -1$, $n = 1, 2$, will yield rational expressions for f, g and h,

$$f = p_0^2\left\{\left[x + \frac{\Omega_0 - \Omega_0^*}{2}it\right]^2 + \left(\frac{\Omega_0 + \Omega_0^*}{2}\right)^2 t^2 + \left(\frac{2}{\Omega_0 + \Omega_0^*}\right)^2\right\} + O\left(p_0^3\right),$$

$$g = p_0^2\left\{\begin{aligned}&\left[x + \frac{\Omega_0 - \Omega_0^*}{2}it\right]^2 + \left(\frac{\Omega_0 + \Omega_0^*}{2}\right)^2 t^2 + \left(\frac{2}{\Omega_0 + \Omega_0^*}\right)^2 \\ &+ \frac{2}{\left|\Omega_0 + 2ki\right|^2}\left[\left(\Omega_0 - \Omega_0^* + 4ki\right)x + \left(\left(\Omega_0^2 + \left(\Omega_0^*\right)^2\right)i - 2k\left(\Omega_0 - \Omega_0^*\right)\right)t - 2\right]\end{aligned}\right\} \\ + O\left(p_0^3\right)$$

$$h = p_0^2\left\{\begin{aligned}&\left[x + \frac{\Omega_0 - \Omega_0^*}{2}it\right]^2 + \left(\frac{\Omega_0 + \Omega_0^*}{2}\right)^2 t^2 + \left(\frac{2}{\Omega_0 + \Omega_0^*}\right)^2 \\ &+ \frac{2}{\left|\Omega_0\right|^2}\left[\left(\Omega_0 - \Omega_0^*\right)x + \left(\Omega_0^2 + \left(\Omega_0^*\right)^2\right)it - 2\right]\end{aligned}\right\} + O\left(p_0^3\right). \tag{14}$$

Consequently rational solutions are obtained as

$$A = \rho \exp\left[i(kx - \omega t)\right]\left\{1 + \frac{\frac{4}{a^2 + (b+2k)^2}\left[(b+2k)ix + (a^2 - b^2 - 2bk)it - 1\right]}{(x-bt)^2 + a^2t^2 + \frac{1}{a^2}}\right\}, \qquad (15)$$

$$B = \rho\left\{1 + \frac{\frac{4}{(a^2+b^2)}\left[bix + (a^2 - b^2)it - 1\right]}{(x-bt)^2 + a^2t^2 + \frac{1}{a^2}}\right\}, \qquad (16)$$

$$L = 4\left\{\frac{1}{(x-bt)^2 + a^2t^2 + \frac{1}{a^2}} - \frac{2(x-bt)^2}{\left[(x-bt)^2 + a^2t^2 + \frac{1}{a^2}\right]^2}\right\}. \qquad (17)$$

where a, b are the real and imaginary parts of the complex angular frequency Ω_0:

$$\Omega_0 = a + ib. \qquad (18)$$

Simple contour plots of such rogue waves for typical values of the parameters exhibit displacements localized in space (x) and time (t) (Figs. 1(a)-1(d)).

4 Amplitude of the rogue wave

Rogue waves of elevation and depression

The maximum amplitude of a rogue wave in an otherwise relatively calm sea state is obviously a factor of interest in the maritime community, and also in other

physical contexts. Analytically this is also a crucial issue as the knowledge gathered reveals valuable structural information concerning these localized entities.

We focus on the exact solution Eqs. (13, 15-18) of Eq. (2). The short wave components are studied first, and one considers the turning points of the function $K(x,t)$,

$$K = \frac{|A|^2}{\rho^2} \text{ where } A \text{ is given by Eq. (15).} \tag{19}$$

At the point $(x,t) = (0,0)$, one has

$$\frac{\partial K}{\partial x} = 0,\ \frac{\partial K}{\partial t} = 0 \text{ with } K(0,0) = \left[1 - \frac{4}{1 + \left(\frac{b+2k}{a}\right)^2}\right]^2.$$

The second order derivatives at (0,0) are

$$\left.\frac{\partial^2 K}{\partial x^2}\right|_{(0,0)} = \frac{48a^6\left[-1 + \left(\frac{b+2k}{a}\right)^2\right]}{\left[a^2 + (b+2k)^2\right]^2},$$

$$\left[\frac{\partial^2 K}{\partial x^2}\frac{\partial^2 K}{\partial t^2} - \left(\frac{\partial^2 K}{\partial x \partial t}\right)^2\right]_{(0,0)} = \frac{768a^{14}}{\left[a^2 + (b+2k)^2\right]^4}\left\{\left[\left(\frac{b+2k}{a}\right)^2 - \frac{5}{3}\right]^2 - \frac{16}{9}\right\}.$$

There are thus three possible scenarios:

(i) For $0 \le \left(\frac{b+2k}{a}\right)^2 < \frac{1}{3}$, (0,0) is a local maximum point with $|A|$ ranging from 3ρ to 2ρ, where again ρ is the amplitude of the background wave;

(ii) For $\frac{1}{3} < \left(\frac{b+2k}{a}\right)^2 < 3$, (0,0) is a saddle point with $|A|$ ranging from 2ρ to 0;

(iii) For $3 < \left(\frac{b+2k}{a}\right)^2$, (0,0) is a local minimum point with $|A|$ ranging from 0 to ρ.

By setting $k = 0$ in the above analysis, we can arrive at similar results for $|B|$.

As the integral $\int L dx$ over the entire domain must be conserved for localized initial conditions, there must be 'elevations' above and 'depressions' below the (zero) mean level. This is verified for the case of a stationary plane wave background. The long rogue wave L, Eq. (17), attains a maximum value of $4a^2$ at (0,0), and a minimum at the points $\left(\pm\frac{\sqrt{3}}{a},0\right)$ with $L\left(\pm\frac{\sqrt{3}}{a},0\right) = -\frac{a^2}{2}$, substantiating the fact that L goes both above and below the (zero) mean level (Fig. 1(c)). These analytic formulations can help to explain the transformation of the wave profiles in the next section [17].

Comparison with the case of a single short wave

It is instructive to compare the present results with that of a single short wave on a stationary background which is studied earlier in the literature. The system Eq. (1) has rogue wave mode [15]:

$$S=\rho_0\left\{1+\frac{-4+2x\left(\Omega_{00}-\Omega_{00}^*\right)+2it\left[\Omega_{00}^2+\left(\Omega_{00}^*\right)^2\right]}{\left|\Omega_{00}\right|^2\left[\left(x+it\frac{\Omega_{00}-\Omega_{00}^*}{2}\right)^2+\left(\frac{\Omega_{00}+\Omega_{00}^*}{2}\right)^2t^2+\left(\frac{2}{\Omega_{00}+\Omega_{00}^*}\right)^2\right]}\right\} \tag{20}$$

where $\Omega_{00}^3=2i\sigma\rho_0^2$, i.e. $\Omega_{00}=\frac{\sqrt[3]{2\sigma\rho_0^2}}{2}\left(\pm\sqrt{3}+i\right)$ or $-\sqrt[3]{2\sigma\rho_0^2}i$. The latter is rejected as Ω_{00} cannot be purely imaginary for a purely imaginary wavenumber, otherwise the solution is singular. Putting $\Omega_{00}=\frac{\mu}{2}\left(\pm\sqrt{3}+i\right)$, where $\mu=\sqrt[3]{2\sigma\rho_0^2}$ into *S*, the intensity of the wave will be given by

$$K_0=\frac{|S|^2}{\rho_0^2}=\frac{\left(\begin{array}{l}9\mu^8t^4-18\mu^7xt^3+27\mu^6t^2x^2-18\mu^5tx^3-12\mu^4t^2\\+9\mu^4x^4+120\mu^3tx-12\mu^2x^2+64\end{array}\right)}{\left(3\mu^4t^2-3\mu^3tx+3\mu^2x^2+4\right)^2}. \tag{21}$$

By elementary algebra, as the expression

$$\left(9\mu^8 t^4 - 18\mu^7 xt^3 + 27\mu^6 t^2 x^2 - 18\mu^5 tx^3 - 12\mu^4 t^2 + 9\mu^4 x^4 + 120\mu^3 tx - 12\mu^2 x^2 + 64\right)$$
$$- 4\left(3\mu^4 t^2 - 3\mu^3 tx + 3\mu^2 x^2 + 4\right)^2$$
$$= -27\mu^2\left[\left(\mu^3 t^2 - \mu^2 tx\right)^2 + \left(\mu^2 tx - \mu x^2\right)^2 + \left(2\mu t - 2x\right)^2 + \mu^4 t^2 x^2\right]$$

is negative, the upper bound of K_0 is thus 4, which is attained at $(x,t) = (0,0)$.

Hence the amplitude of the short wave S will be just two times that of the background plane wave (upper bound of K_0 of Eq. (21) being 4). These analytic formulations can help to explain the transformation of the wave profiles in the next section [17].

Comparison with the nonlinear Schrödinger equation

The Peregrine breather of the nonlinear Schrödinger equation has been widely used as a simple model of a rogue wave, and the maximum amplitude there is three times that of the background plane wave [21]. For a long-short system with one single short wave, this amplification ratio is two. For a long-short system with two short waves, the amplification ratio can be larger than two but will be shown here to be strictly less than three. To establish this fact analytically, it is sufficient to prove that, for Eqs. (15-18), $b \neq 0$ and $b \neq -2k$. Hence we can deduce that both $|A|$ and $|B|$ cannot attain 3ρ at $(x,t) = (0,0)$.

● b is non-zero: Assume the contrary holds, i.e. $\Omega_0 = a$ (real), the dispersion relation then becomes $a^5 - 4k^2a^3 + 8\sigma\rho^2 ka = 0$ and $4ka^4 - 4\sigma\rho^2 a^2 + 8\sigma\rho^2 k^2 = 0$. Eliminating σ will give a contradiction $\left(a^2 + k^2\right)^2 + 7k^4 = 0$ and hence b is non-zero.

● $b \neq -2k$: Assume the contrary holds, i.e. $b = -2k$, the dispersion relation then becomes $a^5 - 12k^2a^3 - 8\sigma\rho^2 ka = 0$, and $-6ka^4 + \left(8k^3 - 4\sigma\rho^2\right)a^2 + 8\sigma\rho^2 k^2 = 0$. Straightforward algebra will give

$$a^2 = \frac{40k^2\sigma\rho_0^2}{-64k^3 - 4\sigma\rho_0^2},$$

and thus σk must be negative. Back substitution yields

$$\left(\sigma\rho_0^2 + 4k^3\right)^2 - \frac{7}{2}\sigma\rho_0^2 k^3 = 0,$$

which is not possible if $\sigma k < 0$, and hence $b \neq -2k$.

Nonlinear coupling enhances the amplitude of the rogue wave

A surprising feature of the nonlinear dynamics of this system is the enhancement of the maximum displacement through coupling. More precisely, the amplitude of the rogue wave of Eq. (2), the system with multiple short waves, can be larger than the corresponding mode in the configuration with just one short

wave. As a concrete example, consider $\rho = 1$, $\sigma = 1$, $k = 1$, $\Omega_0 = 1.15 + 0.569i$ (Fig. 1(b)). From the analysis above, $\left(\frac{b}{a}\right)^2 = 0.245 < \frac{1}{3}$ and hence (0,0) is a maximum point with $|B(0,0)| = 2.22 > 2\rho = 2$. This is greater than the maximum value that the single component model can achieve.

5 Wave profile of the rogue wave mode

Borrowing terminology from optical solitons [2], elevation/depression rogue waves will be labeled as 'bright' and 'dark' respectively in the discussion below.

Profile changes on varying the envelope wavenumber k

For a long-short system with one short wave (Eq. (1)), the rogue wave is always an elevation with a peak value of 2ρ if the background is of zero frequency and of magnitude ρ. For a background with a finite frequency, a depression or 'dark' rogue wave can occur. In terms of varying this frequency parameter, a regime first occurs where the peak is split into two smaller units. The two valleys migrate closer to the original location of single maximum. Eventually the two valleys merge and form the depression/dark rogue wave [17].

The goals of this section are (a) to provide a theoretical description of this splitting and merging process in the coupled system Eq. (2) quantitatively, and (b) to show that the dynamics of multiple waveguides is even richer. For point (a), from the analysis of Section 4, the point (0,0) is a local maximum of $|A|$ for sufficiently small k, implying the occurrence of an ordinary rogue wave mode (Fig. 2(a)). For larger values of k, for example $k = 0.25$ and $\Omega_0 = 1.34 + 0.652i$, one then has $\frac{1}{3} < \left(\frac{b+2k}{a}\right)^2 = 0.738 < 3$ and this maximum splits into two small units which move away from the origin. At the same time, the 'valleys' start to migrate towards the origin, creating a saddle point effect. For still larger values of k ($k = 0.4$), a four-petal type rogue wave is created with $\left(\frac{b+2k}{a}\right)^2 = 1.16$ (Fig. 2(b)). Two maxima and two minima are observed. When k reaches about 0.5 (more precisely $\left(\frac{b+2k}{a}\right)^2 = 1.56 < 3$ with $\Omega_0 = 1.26 + 0.575i$), the two depression petals join together to form a double-depression rogue wave. Finally, the two valleys actually merge and become a single depression/dark rogue wave mode, turning (0,0) into a minimum point. This is illustrated by Fig. 1(a), when k reaches 1 with $\Omega_0 = 1.15 +$

$0.569i$ and thus $\left(\frac{b+2k}{a}\right)^2 = 4.98 > 3$. The analysis of Section 4 shows that the short wave A has become a dark rogue wave with the minimum point at (0,0).

In all of the above cases, B and L remain essentially bright rogue waves. The solution for $k = 1$ is illustrated in Fig. 1. A similar trend can be observed when $\rho = 1$, $\sigma = -1$, with B changing from a bright rogue wave to a dark rogue wave while A maintaining essentially as a bright rogue wave.

Exotic combination of modes

Furthermore, rogue wave modes of the short wave components A and B can have various exotic combinations: bright-bright (Fig. 2(a) and the corresponding diagram for B (not shown)), dark-dark (Figs. 3(a), 3(b)), bright-dark (Figs. 3(c), 3(d)), and dark-bright (Figs. 1(a), (1b)).

Obviously, the form of the rogue wave mode depends on the parameters ρ, σ, k and the value of Ω_0 from the dispersion relation. With given values of ρ, σ and k, different roots of Ω_0 from the quintic dispersion relation can give different types of solutions. In Figs. 1(a) and 1(b), A is a dark rogue wave and B is a bright rogue wave; whereas in Figs. 3(a) and 3(b), both A and B are dark rogue waves. The

values of ρ, σ and k are the same in these two cases but different choices of Ω_0 have been applied.

6 Modulation instability, rogue waves and numerical simulations

Finally it is valuable to investigate the relationship between modulation instability (MI) and the evolution of rogue wave modes with perturbed initial conditions. For MI, one starts with the plane (or continuous) wave solution of Eq. (2) (L_0 = a real constant):

$$A = \rho \exp[ikx - i(L_0 - k^2)t],\ B = \rho \exp(-iL_0 t),\ L = L_0 .$$

Imposing sinusoidal perturbations and isolating modal dependence of

$$\exp[irx - ist]$$

will give a dispersion relation

$$\begin{aligned} & s^5 + 4krs^4 + \left(-2r^4 + 4k^2r^2\right)s^3 + \left(-4kr^5 + 4\sigma\rho^2 r^3\right)s^2 \\ & + \left(8\sigma\rho^2 kr^4 - 4k^2r^6 + r^8\right)s - 4\sigma\rho^2 r^7 + 8\sigma\rho^2 k^2 r^5 = 0 \end{aligned} \quad . \tag{22}$$

For a real wavenumber r, complex roots for angular frequency s will imply instability. In principle this analysis needs to be performed for all r, assuming σ, ρ and k are given. However, from past experience, a disturbance of long wavelength

($0 < r << 1$) tends to constitute an unstable regime. With that assumption, the speed $c = \frac{s}{r}$ for small r will satisfy the equation

$$\Psi(c) = c^5 + 4kc^4 + 4k^2c^3 + 4\sigma\rho^2c^2 + 8\sigma\rho^2kc + 8\sigma\rho^2k^2 = 0. \quad (23)$$

Remarkably, this is identical to Eq. (13) if one makes the transformation

$$\Omega_0 = ic. \quad (24)$$

In hindsight, these equations provide a quantitative correlation between modulation instability and the occurrence of rogue waves. In fact the formulations of Eq. (8) and Eq. (12) show that the speed of a breather should be given by $\frac{p_0\Omega_0}{ip_0}$ which is equal to c by Eq. (24). The condition for the existence of rogue wave is thus identical to the criterion for modulation instability for disturbances of long wavelength.

To substantiate these ideas, numerical simulations have been performed to test whether the occurrence of rogue wave is a robust process. As there are several parameters present and the MI analysis has only been implemented for long wavelength disturbance, we shall only present a few representative cases. The exact solution perturbed by a localized noise with a maximum of 0.1, in a background of magnitude one ($\rho = 1$), was used as the initial condition. Numerical

simulations were carried out with spectral discretization in the spatial domain and a fourth order Runge-Kutta scheme in the temporal domain. The size of the spatial domain was chosen to be from –400 to +400 in both cases presented here. For certain favorable parameter regimes, inherently occurring noise in the surrounding does not essentially affect the 'growth phase' of the rogue wave (Fig. 4). However, in other unfavorable parameter regimes, this 'growth phase' is significantly distorted by the perturbations in the initial conditions (Fig. 5), and other instabilities of the system overwhelm the occurrence of the rogue wave mode.

7 Multi-component System

The analysis of the previous sections can be generalized to a multi-component long wave-short wave model with three or more short wave components. The short wave envelopes S_j , $j = 1, 2,\ldots n$ and the generalized long wave Q will then satisfy

$$i\left(S_j\right)_t - \left(S_j\right)_{xx} = QS_j, \quad \text{for } j = 1, \ldots, n,$$

$$Q_t = -\left(\sum_{j=1}^{n} \sigma_j \left|S_j\right|^2\right)_x, \tag{25}$$

where σ_j measures the nonlinearity and can be normalized numerically to positive or negative unity by scaling the short wave envelopes. An intriguing exercise in nonlinear dynamics then is to consider the case where the signs of the intensity

terms take up various combinations of +1 and –1. However, for simplicity, similar to what we have accomplished in the case discussed earlier for $n = 2$, we restrict attention to $\sigma_j = \sigma$, $j = 1 \ldots n$, and will study other combinations in the future.

An elegant feature of Eq. (25) is that the intensity of each component summed over the entire spatial domain is conserved [22]:

$$\int_{-\infty}^{\infty} |S_j|^2 dx = \text{constant.}$$

Dynamics and properties of solitons in such long wave-short wave systems in two spatial dimensions have been studied in the literature [22, 23], where the Hirota bilinear transform is also employed. Painlevé analysis has been performed to confirm the 'integrability' of the system [22]. Head-on and overtaking collisions, as well as energy distribution properties, are investigated [22, 23]. Mixed (bright-dark) families of solitons are derived theoretically, including cases where the coefficients of nonlinearity are not of a uniform sign [24]. In terms of rogue waves, rational solutions of Eq. (25) have been derived [22, 25], and the geometry of the wavefront in two spatial dimensions has been elucidated. Here we shall further enhance the theoretical understanding by performing the modulation instability analysis. To highlight the nonlinear dynamics with minimal algebraic complexity, the special case with $n = 3$ will be discussed:

$$i\left(S_j\right)_t-\left(S_j\right)_{xx}=QS_j, \quad \text{for } j=1,2,3,$$

$$Q_t=-\sigma\left(\sum_{j=1}^{3}\left|S_j\right|^2\right)_x. \tag{26}$$

The formulation and methodology are similar to those described in Sections 2 and 3. Two arbitrary wavenumbers for the background plane waves can be allowed in general but the symmetrical case is sufficient to illustrate the features of coupling. Along this line of reasoning, the rogue waves for $n = 3$ are given by

$$S_1=\rho\exp\left[i\left(kx+k^2t\right)\right]\left\{1+\frac{\frac{4}{(a')^2+(b'+2k)^2}\left[(b'+2k)ix+\left((a')^2-(b')^2-2b'k\right)it-1\right]}{\left[(x-b't)^2+(a')^2t^2+\frac{1}{(a')^2}\right]}\right\}, \tag{27}$$

$$S_2=\rho\left\{1+\frac{\frac{4}{(a')^2+(b')^2}\left[b'ix+\left((a')^2-(b')^2\right)it-1\right]}{\left[(x-b't)^2+(a')^2t^2+\frac{1}{(a')^2}\right]}\right\}, \tag{28}$$

$$S_3=\rho\exp\left[i\left(-kx+k^2t\right)\right]\left\{1+\frac{\frac{4}{(a')^2+(b'-2k)^2}\left[(b'-2k)ix+\left((a')^2-(b')^2+2b'k\right)it-1\right]}{\left[(x-b't)^2+(a')^2t^2+\frac{1}{(a')^2}\right]}\right\}, \tag{29}$$

$$Q = \frac{4}{\left[(x-b't)^2 + (a')^2 t^2 + \frac{1}{(a')^2}\right]} - \frac{8(x-b't)^2}{\left[(x-b't)^2 + (a')^2 t^2 + \frac{1}{(a')^2}\right]^2}, \quad (30)$$

where $\Omega_0' = a' + ib'$ and Ω_0' satisfies the dispersion relation,

$$\left(\Omega_0'\right)^7 + 8k^2\left(\Omega_0'\right)^5 - 6\sigma\rho^2 i\left(\Omega_0'\right)^4 + 16k^4\left(\Omega_0'\right)^3 - 32\sigma\rho^2 k^4 i = 0. \quad (31)$$

For a system with n short wave envelopes, this dispersion relation will be a polynomial of degree $2n + 1$. Properties similar to those discussed in Sections 4 through 6 can be observed:

- *Coupling can enhance the amplitude of the rogue waves*

  As discussed in Section 4, the peak of any bright rogue wave for system (2) must be less than 3ρ for the short wave components (ρ = background plane wave). In the presence of a third short wave component, the maximum amplitude can be three times the background amplitude ρ for one of the short wave components. As an illustrative example, for σ = 0.1, ρ = 1, k = 10, the maximum displacement of $|S_3|$ is 3, whereas the other components have insignificant variations in amplitude.

- *Multiple rogue wave modes*

  The degree of the dispersion relation Eq. (31) is higher than that of the dispersion relation Eq. (13) for system (2) by two. In certain parameter regime, three distinct sets of rogue wave solutions will be possible. A typical case is illustrated in Figs. 6-8: S_3 can be a bright, four-petal type or dark rogue wave depending on the value of the root Ω_0'.

- *Connection with modulation instability*

  The connection between existence of rogue waves and the onset of modulation instability can be drawn. Consider the plane wave solution of system (26):

  $$S_1 = \rho \exp\left[i\left(kx + k^2 t\right)\right],\ S_2 = \rho,\ S_3 = \rho \exp\left[i\left(-kx + k^2 t\right)\right],\ Q = 0.$$

  Imposing sinusoidal perturbations of the form $\exp[i(Kx - Wt)]$ to the plane wave solution, the angular frequency of these disturbances is given by

  $$\begin{aligned} &W^7 - \left(3K^4 + 8k^2K^2\right)W^5 + 6\sigma\rho^2K^3W^4 + \left(3K^8 + 16k^4K^4\right)W^3 \\ &-12\sigma\rho^2K^7W^2 + \left(-K^{12} + 8k^2K^{10} - 16k^4K^8\right)W \\ &+\sigma\rho^2\left(6K^{11} - 32k^2K^9 + 32k^4K^7\right) = 0. \end{aligned}$$

  With $c' = \dfrac{W}{K}$, this governing equation for the angular frequency becomes

$$(c')^7 - 8k^2(c')^5 + 6\sigma\rho^2(c')^4 + 16k^4(c')^3 + 32\sigma\rho^2k^4 = 0 \qquad (32)$$

in the limit for vanishingly small K. This kind of instability for complex roots of Eq. (32), with special restriction to disturbances with vanishingly small wavenumbers, has been termed baseband modulation instability. This instability was demonstrated to be related to the occurrence of rogue waves [26]. By the transformation $\Omega_0' = ic'$, Eq. (31) is mapped to Eq. (32). In other words, the existence condition of rogue waves (Eqs. (27-30)) is equivalent to the condition for long wavelength instability. Physically, baseband modulation instability is necessary for rogue waves to occur in this coupled system.

We have thus utilized the cases with two and three short wave envelopes to illustrate a very rich and elegant dynamical system of long wave-short wave resonance with n components.

8 Conclusions

Rogue waves are unexpectedly large displacements from an otherwise calm background, and have generated intense scientific interest as such modes occur in many physical contexts [6]. Rogue waves for a nonlinear coupled system Eq. (2) of

long wave-short wave interactions are obtained analytically as algebraic modes localized in both space and time. Besides documenting an analytical solution to a nonlinear evolution system, the results and techniques of the present work are potentially applicable in fields beyond the problem of long wave-short wave resonance through these perspectives:

● Instead of the widely used Darboux transformation, rogue waves here are obtained as a long wave limit of a breather/multi-soliton expression obtained from the Hirota bilinear transformation [15]. As the Hirota bilinear forms for most integrable equations are known [22-25], this opens an alternative and fruitful path for calculating rogue wave modes.

● A remarkable property of nonlinear dynamics in multiple waveguides is demonstrated, by showing that the maximum displacements of the rogue waves in a system with multiple short waves can be larger than that of the rogue wave mode in a configuration with just one short wave. Multiple configurations of rogue wave modes for a fixed set of input parameters are also possible [27].

● Rogue waves of a nonlinear evolution system can occur as an elevation (above the mean level) or a depression (below the mean level), depending on the values of the relevant parameters. An analytical description of this transition is offered here,

starting from the splitting of a peak, through the migration of the adjacent valleys, and finally the merger of these valleys to form a depression rogue wave [27, 28].

● The connection between the existence criterion of rogue waves and the onset of baseband modulation instability is confirmed [26].

● Exotic combinations of modes, e.g. bright-dark or dark-dark rogue waves are calculated in closed form.

However, there are still other challenges ahead. Theoretically, the Lax pair of the coupled system has been formulated, but investigations of the full analytical structures have not been completed. Physically, studies of higher order rogue wave modes have been initiated [25], but computational studies of their stability have not been undertaken [29]. A comprehensive study on the structural stability of these modes will yield further information on this dynamical system. Furthermore, the interactions between solitons and rogue waves will constitute an intriguing nonlinear dynamical system [22, 30, 31]. These and other issues await future efforts.

Acknowledgement

D.J.K. acknowledges the support from the Australian Research Council (Discovery Project No. DP110102068). Partial financial support for the present

research team has been provided by the Research Grants Council General Research Fund contracts HKU711713E and HKU17200815.

References

[1] Craik, A.D.D.: Wave Interactions and Fluid Flows. Cambridge University Press, New York (1985).

[2] Kivshar, Y.S., Agrawal, G.: Optical Solitons: From Fibers to Photonic Crystals. Academic Press, San Diego (2003).

[3] Benney, D.J.: Significant interactions between small and large scale surface waves, Stud. Appl. Math. **55**, 93 (1976).

[4] Ma, Y.C.: The complete solution of the long-wave-short-wave resonance equations, Stud. Appl. Math. **59**, 201 (1978).

[5] Ma, Y.C., Redekopp, L.G.: Some solutions pertaining to the resonant interaction of long and short waves, Phys. Fluids **22**, 1872 (1979).

[6] Onorato, M., Residori, S., Bortolozzo, U., Montina, A., Arecchi, F.T.: Rogue waves and their generating mechanisms in different physical contexts, Phys. Rep. **528**, 47 (2013).

[7] Ivancevic, V.G., Reid, D.J.: Turbulence and shock waves in crowd dynamics, Nonlinear Dyn. **68**, 285 (2012).

[8] Zhu, H.P.: Nonlinear tunneling for controllable rogue waves in two dimensional graded-index waveguides, Nonlinear Dyn. **72**, 873 (2013).

[9] Akhmediev, N., Ankiewicz, A., Soto-Crespo, J.M.: Rogue waves and rational solutions of the nonlinear Schrödinger equation, Phys. Rev. E **80**, 026601 (2009).

[10] Bludov, Yu.V, Konotop, V.V., Akhmediev, N.: Vector rogue waves in binary mixtures of Bose-Einstein condensates, Eur. Phys. J. Special Topics **185**, 169 (2010).

[11] Vinayagam, P.S., Radha, R., Porsezian, K.: Taming rogue waves in vector Bose-Einstein condensates, Phys. Rev. E **88**, 042906 (2013).

[12] Zhao, L.C., Liu, J.: Localized nonlinear waves in a two-mode nonlinear fiber, J. Opt. Soc. Am. B **29**, 3119 (2012).

[13] Yan, Z.: Vector financial rogue waves, Phys. Lett. A **375**, 4274 (2011).

[14] Zhai, B.G., Zhang W.G., Wang, X.L., Zhang, H.Q.: Multi-rogue waves and rational solutions of the coupled nonlinear Schrödinger equations, Nonlinear Anal. – Real World Appl. **14**, 14 (2013).

[15] Chow, K.W., Chan, H.N., Kedziora, D.J., Grimshaw, R.H.J.: Rogue wave modes for the long wave-short wave resonance model, J. Phys. Soc. Jpn. **82**, 074001 (2013).

[16] Matsuno, Y.: Bilinear Transformation Method. Academic Press, Orlando (1984).

[17] Chen, S., Grelu, P., Soto-Crespo, J.M.: Dark- and bright-rogue-wave solutions for media with long-wave-short-wave resonance, Phys. Rev. E **89**, 011201(R) 2014.

[18] Dudley, J.M., Genty, G., Dias, F., Kibler, B., Akhmediev, N.: Modulation instability, Akhmediev breathers and continuous wave supercontinuum generation, Opt. Expr. **17**, 21497 (2009).

[19] Ma, Y.C.: The resonant interaction among long and short waves, Wave Motion **3**, 257 (1981).

[20] Kedziora, D. J., Ankiewicz, A., Akhmediev, N.: Classifying the hierarchy of nonlinear-Schrödinger-equation rogue wave solutions, Phys. Rev. E **88**, 013207 (2013).

[21] Shrira, V.I., Geogjaev, V.V.: What makes the Peregrine soliton so special as a prototype of freak waves?, J. Eng. Math. **67**, 11 (2010).

[22] Sakkaravarthi, K., Kanna, T., Vijayajayanthi, M., Lakshmanan, M.: Multicomponent long-wave-short-wave resonance interaction system: Bright solitons, energy-sharing collisions, and resonant solitons, Phys. Rev. E **90**, 052912 (2014).

[23] Kanna, T., Vijayajayanthi, M., Sakkaravarthi, K., Lakshmanan, M.: Higher dimensional bright solitons and their collisions in a multicomponent long wave-short wave system, J. Phys. A: Math. Theor. **42**, 115103 (2009).

[24] Chen, J., Chen, Y., Feng, B.-F., Maruno, K.: General mixed multi-soliton solutions to one-dimensional multicomponent Yajima-Oikawa system, J. Phys. Soc. Jpn. **84**, 074001 (2015).

[25] Chen, J., Chen, Y., Feng, B.-F., Maruno, K.: Rational solutions to two- and one-dimensional multicomponent Yajima-Oikawa systems, Phys. Lett. A **379**, 1510 (2015).

[26] Baronio, F., Conforti, M., Degasperis, A., Lombardo, S., Onorato, M., Wabnitz, S.: Vector rogue waves and baseband modulation instability in the defocusing regime, Phys. Rev. Lett. **113**, 034101 (2014).

[27] Chen, S., Soto-Crespo, J. M., Grelu, P.: Coexisting rogue waves within the (2+1)-component long-wave-short-wave resonance, Phys. Rev. E **90**, 033203 (2014).

[28] Li, J. H., Chan, H. N., Chiang, K. S., Chow, K. W.: Breathers and 'black' rogue waves of coupled nonlinear Schrödinger equations with dispersion and nonlinearity of opposite signs, Commun. Nonlinear Sci. Numer. Simulat. **28**, 28 (2015).

[29] Chan, H. N., Malomed, B. A., Chow, K. W., Ding, E.: Rogue waves for a system of coupled derivative nonlinear Schrödinger equations, Phys. Rev. E **93**, 012217 (2016).

[30] Kanna, T., Vijayajayanthi, M., Lakshmanan, M.: Mixed solitons in a (2+1)-dimensional multicomponent long-wave-short-wave system, Phys. Rev. E **90**, 042901 (2014).

[31] Baronio, F., Degasperis, A., Conforti, M., Wabnitz, S.: Solutions of the vector nonlinear Schrödinger equations: evidence for deterministic rogue waves, Phys. Rev. Lett. **109**, 044102 (2012).

Figures Captions

Fig. 1 Contour plots of (a) the norm of the short wave component A, (b) the norm of the short wave component B, and (c) the long wave component L, of the exact solutions Eqs. (15-17) on the x-t plane; (d) a three dimensional plot of the short wave component $|B|$; values for the parameters: $\rho = 1$, $\sigma = 1$, $k = 1$, $\Omega_0 = 1.15 + 0.569i$. A is a dark rogue wave and B is a bright rogue wave with a maximum value greater than 2ρ. L is a bright rogue wave with two minimum points with negative values

Fig. 2 Contour plots of the norm of the short wave component A for $\rho = 1$, $\sigma = 1$, and (a) $k = 0$, $\Omega_0 = 1.37 + 0.794i$; (b) $k = 0.4$, $\Omega_0 = 1.30 + 0.597i$. The peak at (0,0) splits as k increases

Fig. 3 Contour plots of (a) the norm of the short wave component A, and (b) the norm of the short wave component B for $\rho = 1$, $\sigma = 1$, $k = 1$, $\Omega_0 = 0.637 - 1.13i$, which is a dark-dark combination. Contour plots of (c) the norm of the short wave component A, and (d) the norm of the short wave component B for $\rho = 1$, $\sigma = -1$, $k = 1$, $\Omega_0 = 0.894 - 2.12i$, which is a bright-dark combination

Fig. 4 An example of robust occurrence of rogue waves: Initial noise disturbances do not essentially affect the 'growth phase' of the rogue wave: $\rho = 0.25$, $\sigma = 1$, $k = 1$, $\Omega_0 = 0.436 + 0.243i$

Fig. 5 An example of the unstable nature of rogue waves: Initial noise disturbances can significantly distort the 'growth phase' of the rogue wave: $\rho = 1$, $\sigma = 1$, $k = 1.25$, $\Omega_0 = 0.552 - 1.430i$

Fig. 6 Contour plots of the norm of the short wave component (a) S_1 (dark), (b) S_2 (dark), (c) S_3 (bright), and (d) the long wave component Q (bright), of the exact solutions Eqs. (27-30) on the x-t plane; values for the parameters: $\rho = 1$, $\sigma = 1$, $k = 1$, $\Omega_0' = -0.883 + 2.1i$

Fig. 7 Contour plots of the norm of the short wave component (a) S_1 (dark), (b) S_2 (bright), (c) S_3 (four-petal), and (d) the long wave component Q (bright), of the exact solutions Eqs. (27-30) on the x-t plane; values for the parameters: $\rho = 1$, $\sigma = 1$, $k = 1$, $\Omega_0' = -0.973 + 0.504i$

Fig. 8 Contour plots of the norm of the short wave component (a) S_1 (four-petal), (b) S_2 (dark), (c) S_3 (dark), and (d) the long wave component Q (bright), of the exact solutions Eqs. (27-30) on the x-t plane; values for the parameters: $\rho = 1$, $\sigma = 1$, $k = 1$, $\Omega_0' = -0.661 - 1.16i$

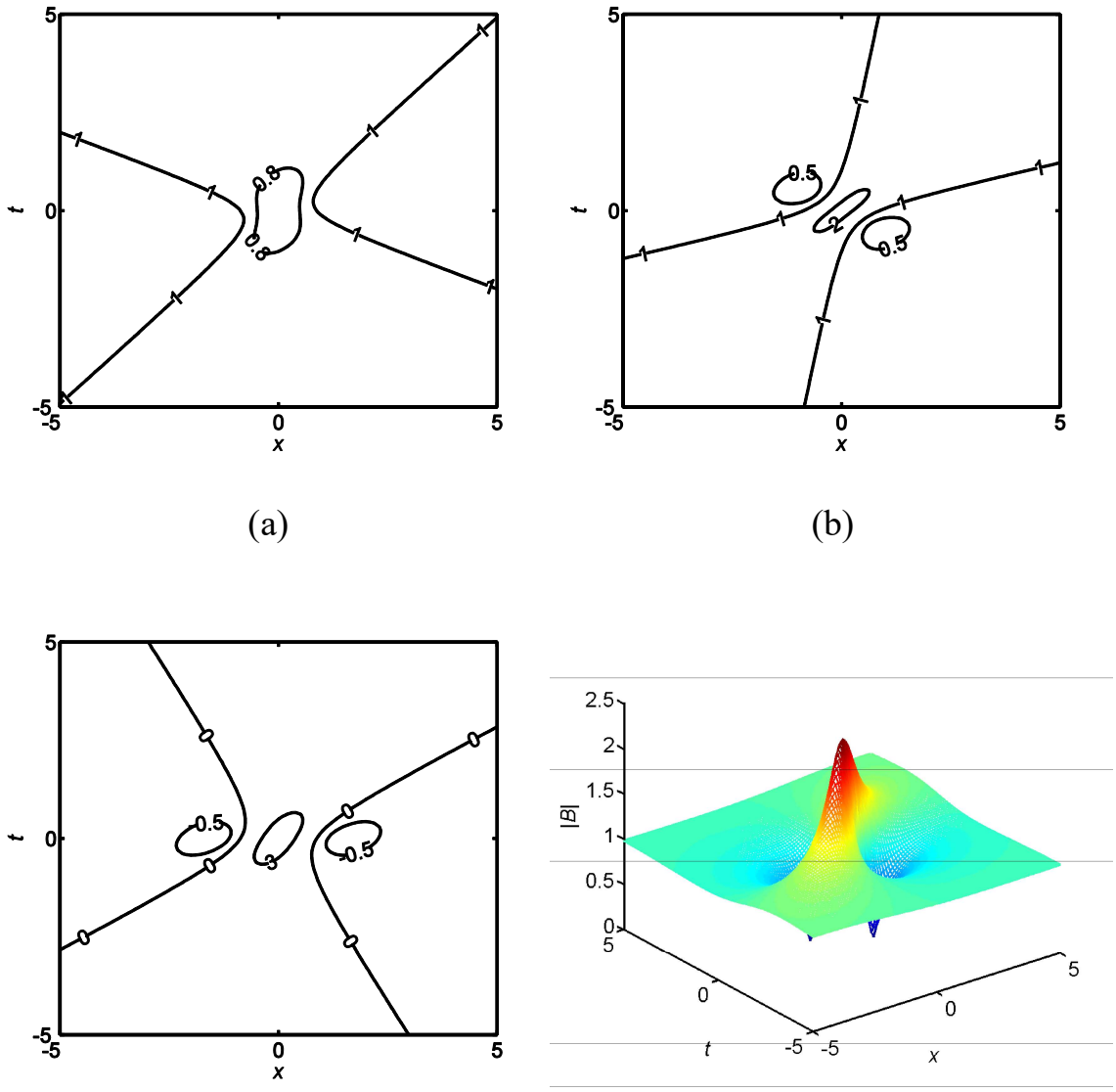

Figure 1

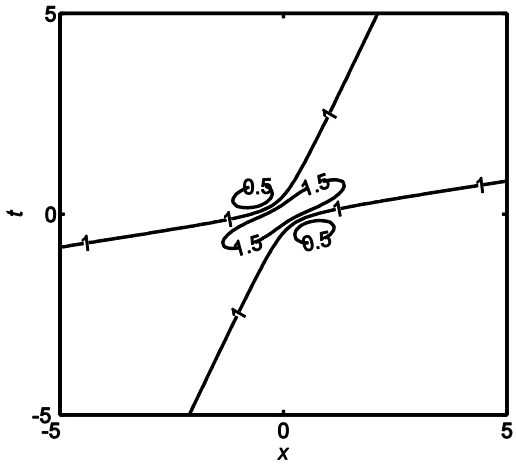

(a)

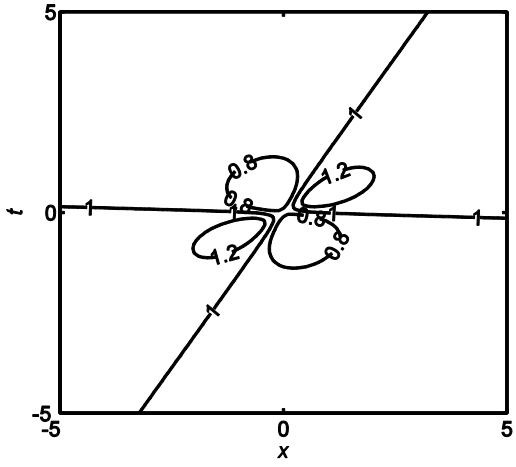

(b)

Figure 2

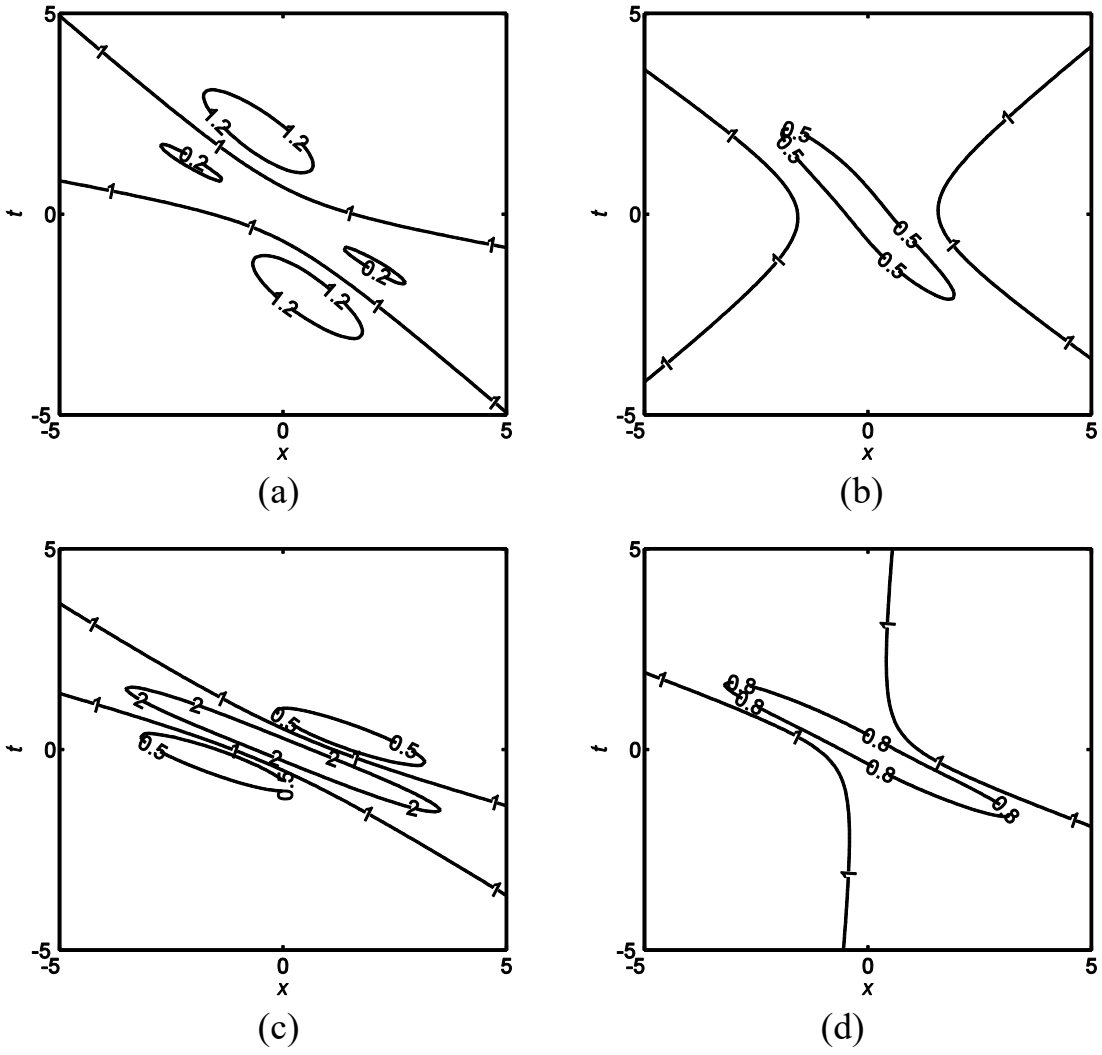

Figure 3

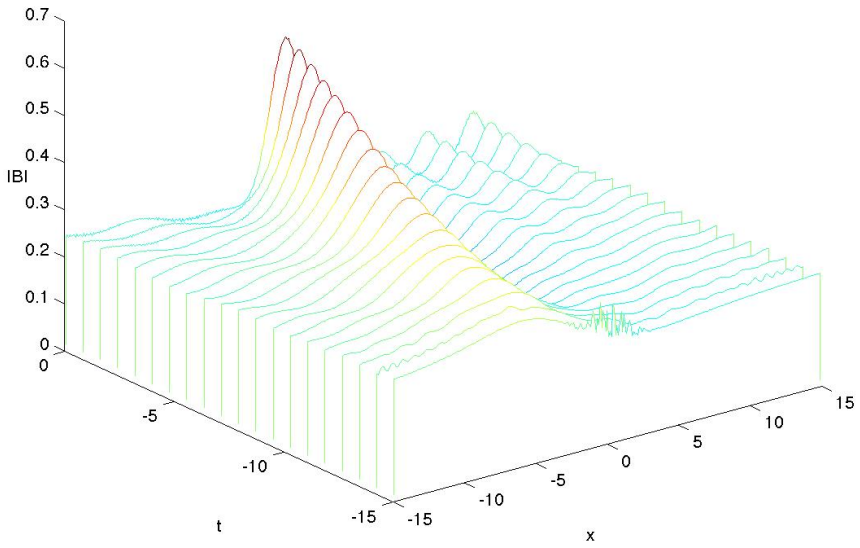

Figure 4

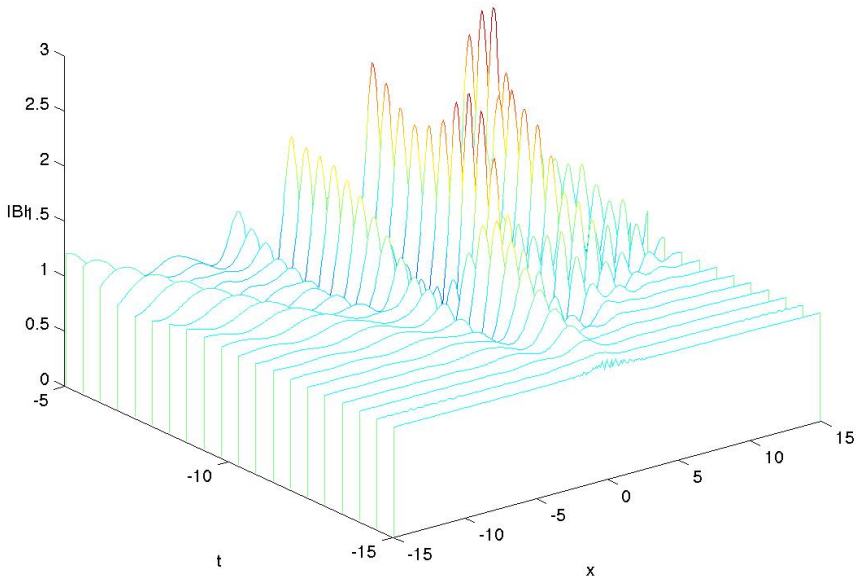

Figure 5

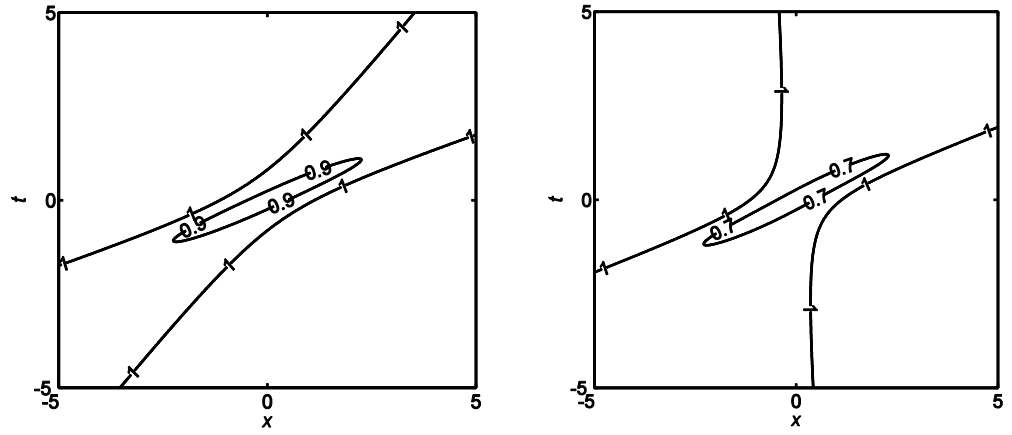

(a) (b)

(c) (d)

Figure 6

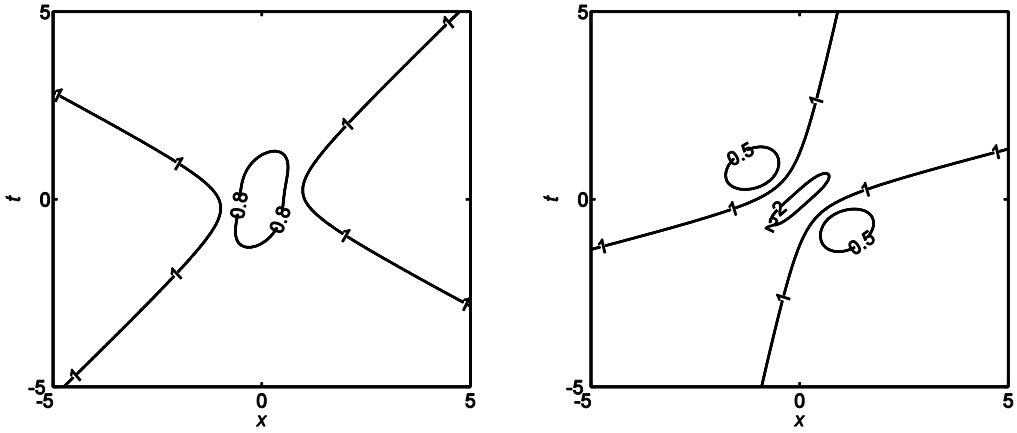

(a) (b)

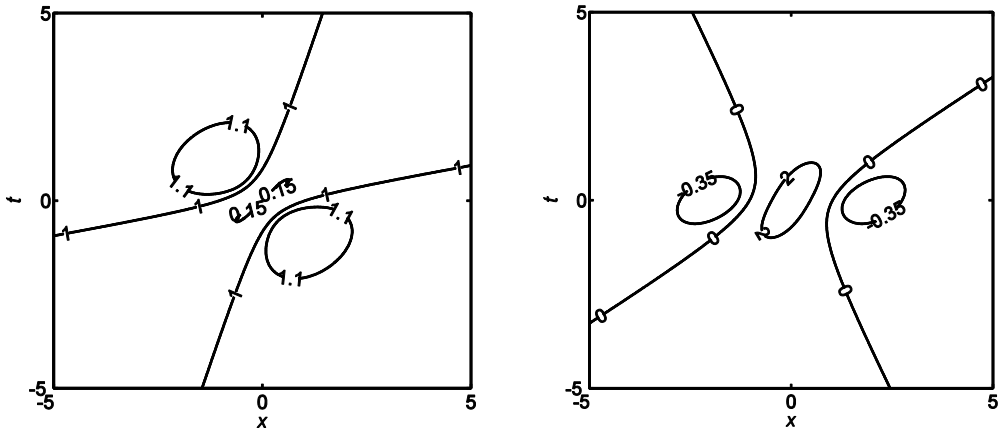

(c) (d)

Figure 7

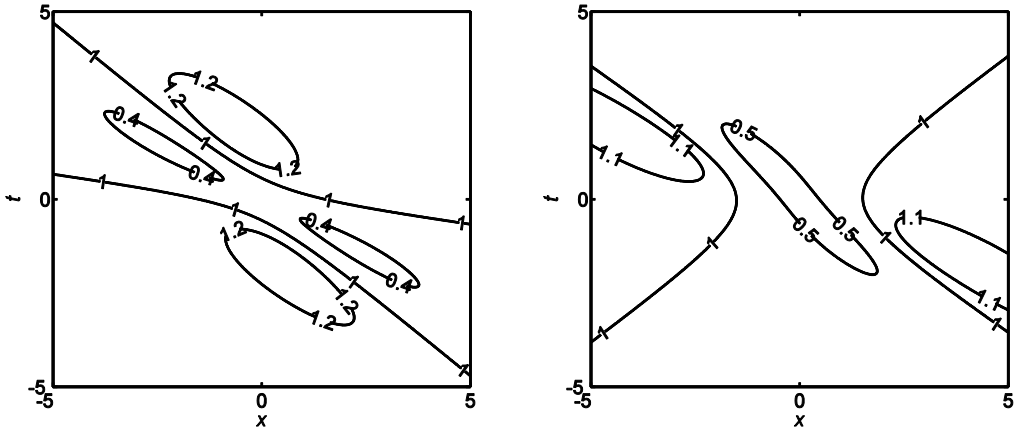

(a) (b)

(c) (d)

Figure 8